DNA Nanotechnology

International Edition: DOI: 10.1002/anie.201610133
German Edition: DOI: 10.1002/ange.201610133

Cuboid Vesicles Formed by Frame-Guided Assembly on DNA Origami Scaffolds

Yuanchen Dong, Yuhe Renee Yang, Yiyang Zhang, Dianming Wang, Xixi Wei, Saswata Banerjee, Yan Liu, Zhongqiang Yang, Hao Yan, and Dongsheng Liu**

Abstract: *We describe the use of a frame-guided assembly (FGA) strategy to construct cuboid and dumbbell-shaped hetero-vesicles on DNA origami nanostructure scaffolds. These are achieved by varying the design of the DNA origami scaffolds that direct the distribution of the leading hydrophobic groups (LHG). By careful selection of LHGs, different types of amphiphiles (both polymer and small-molecule surfactants) were guided to form hetero-vesicles, demonstrating the versatility of the FGA strategy and its potential to construct asymmetric and dynamic hetero-vesicle assemblies with complex DNA nano-scaffolds.*

Amphiphilic molecules have the tendency to self-assemble into morphologies with smooth surfaces, such as spherical micelles,[1] fibers,[2] tubes,[3] and vesicles,[4] to minimize the surface tension and thus the Gibbs free energy, which is consistent with the second law of thermodynamics.[5] The natural tendency to achieve the most thermally stable states makes it challenging to construct cuboid amphiphilic assemblies, in which the free energy is not minimized. Recently, inspired by the cytoskeletal-membrane protein-lipid bilayer system,[6] we have proposed a frame-guided assembly (FGA) strategy, which in principle can be used to construct hetero-vesicles, composed of leading molecules and the principal amphiphiles (PA), with customized shapes and sizes in an identical environment.[7] To date, using gold nanoparticle/DNA as scaffolds, only sphere- and rod-shaped amphiphilic assemblies have been created.[8] Herein, taking advantage of the geometric programmability of DNA origami nanostructures,[9] we demonstrated the construction of hetero-vesicles with cuboid and dumbbell shapes, demonstrating the generality of the FGA strategy in guiding the formation of geometrically challenging amphiphilic assemblies.

The FGA process using a cuboid scaffold is illustrated in Figure 1. DNA origami cuboid **1** is used as a model scaffold to show the compatibility between the DNA nanotechnology and FGA strategy. The dimensions of cuboid **1** are approximately 20 nm × 20 nm × 40 nm, and in total, 115 copies of polyA strands (A_{20} extended out of the DNA origami) were modified on its surfaces with an average inter-molecular distance of 5–7 nm. The poly(aryl ether) dendron, which has a hydrophobic core and carries eight hydrophilic oligo(ethylene glycol) (OEG) tails to increase the solubility of the molecule in an aqueous solution, was selected as the leading hydrophobic group (LHG). The dendron was covalently linked to a polyT strand (T_{20}) to form the conjugate D_TDOEG. The polyT tail brought the dendron onto the surface of the DNA origami upon hybridization with the polyA strands distributed on the surfaces of the cuboid DNA origami to form the amphiphilic frame. When the principal amphiphile (PA) G_2Cl-18 molecules are added, they are guided by the LHG to assemble along the surfaces of the frame to fill in the gaps between the LHG and to close in on themselves to form a hetero-vesicle, with its external morphology following that of the cuboid DNA origami scaffold. The D_TDOEG and G_2Cl-18 molecules were synthesized by a solid-phase conjugation as described previously,[7a] and the

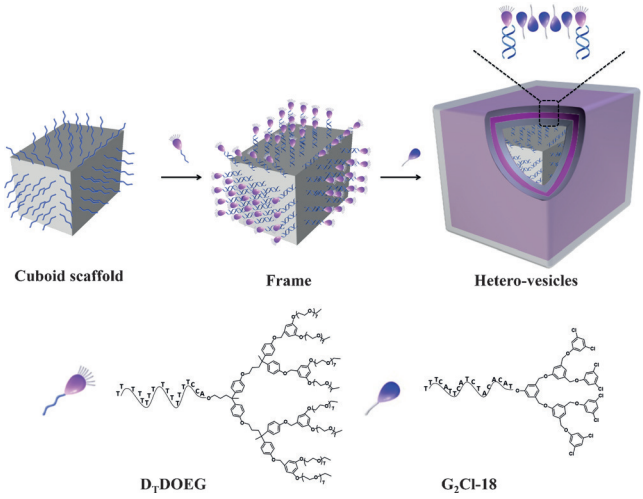

Figure 1. Schematic of the frame-guided assembly process with a DNA origami scaffold. The cuboid origami was designed with 115 ssDNA polyA (A_{20}) extensions to allow the polyT-amphiphilic DDOEG dendron conjugated molecule, D_TDOEG, to be anchored to the origami by DNA hybridization, which acts as the leading hydrophobic group to guide the assembly of the principle amphiphile, G_2Cl-18. Upon the addition of G_2Cl-18, the leading hydrophobic groups on the surfaces of the frame guide G_2Cl-18 to fill the gaps between them by interactions with the hydrophobic dendron domain to complete the formation of the hetero-vesicles around the frame.

[*] Dr. Y. Dong, Y. Zhang, D. Wang, Dr. Z. Yang, Dr. D. Liu
Key Laboratory of Organic Optoelectronics & Molecular Engineering of the Ministry of Education, Department of Chemistry, Tsinghua University
Beijing 100084 (China)
E-mail: liudongsheng@tsinghua.edu.cn
Dr. Y. R. Yang, Dr. X. Wei, S. Banerjee, Dr. Y. Liu, Dr. H. Yan
School of Molecular Sciences and Center of Molecular Design & Biomimetics at Biodesign Institute, Arizona State University
Tempe, AZ 85287 (USA)
E-mail: hao.yan@asu.edu

Supporting information for this article can be found under: http://dx.doi.org/10.1002/anie.201610133.

sequence information can be found in the Supporting Information.

Cuboid **1** was constructed through the DNA origami strategy as previously reported.[10] The detailed staple strand information and the annealing procedure can be found in the Supporting Information. The transmission electron microscopy (TEM) images showed well-formed cuboid assemblies (Figure 2a), which revealed the successful formation of the DNA scaffold. The formation of cuboid **1** was also confirmed by 1% agarose gel electrophoresis (Supporting Information, Figure S1, lane 2).

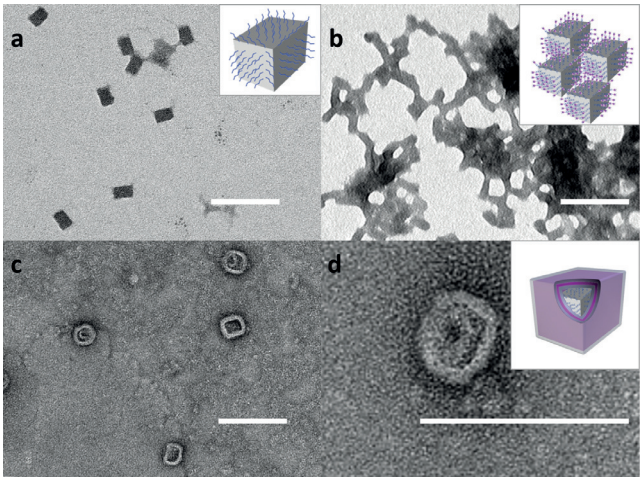

Figure 2. TEM analysis of the assemblies. a) The DNA origami cuboid **1**. b) The frame aggregates formed by the hybridization of cuboid **1** and D_TDOEG. c,d) Hetero-vesicles with the addition of 5 μM G_2Cl-18. Samples are negatively stained with uranyl acetate. Scale bars = 100 nm.

It should be noted that during the preparation of the DNA origami, a high concentration of Mg^{2+} is necessary, which may have undesired interactions with the DNA tail of the G_2Cl-18 molecules and affect its assembly. To avoid the influence of Mg^{2+} in the amphiphilic assembly process, we changed the DNA origami buffer solution from the TAE Mg^{2+} buffer to a 0.5 × TBE buffer containing no Mg^{2+} but 200 mM NaCl. The buffer exchange was performed by ultrafiltration and washing using a molecular cutoff (100 K) filtration device after the formation of the DNA cuboids. Even after weeks of buffer exchange, the DNA cuboid kept its cuboid shape and was able to hybridize with D_TDOEG. It was noted that when we use the full complimentary T20 strand to hybridize with the A20 extensions on the DNA origami, the DNA cuboid aggregated, possibly because of the π–π stacking (data not shown). To avoid this aggregation, we introduced an extra three-nucleotide overhang at the 5′-end of the T20 sequence, as shown in the Supporting Information, Table S1, and the same sequenced overhang was also introduced to the polyT tail of D_TDOEG. The hybridization of cuboid **1** and T23 showed low or no aggregation (Supporting Information, Figure S1, lane 3). For the FGA process, in a typical experiment, a 4 nM solution of cuboid **1** was incubated with 2 μM D_TDOEG (a 4-fold excess in the polyA strands available) to form the frame at 4 °C for 3 h in 0.5 × TBE, 200 mM NaCl. The frame hybridized with D_TDOEG showed much lower mobility and could not run out of the gel well under the same electrophoresis conditions used (Supporting Information, Figure S1, lane 4). This revealed the aggregation of the frames upon decoration of the LHGs.

To monitor the assembly process, SYBR Green I, which exhibits green fluorescence after binding with duplex DNA under UV excitation, was added to the incubation solution. The precipitation observed under 254-nm UV light displayed green fluorescence (Supporting Information, Figure S2b) indicating the presence of the DNA nanostructures. With the addition of 5 μM G_2Cl-18 and after a short annealing procedure from 37 °C to 25 °C, the precipitation disappeared and the solution turned back to a clear solution (Supporting Information, Figure S2c). This observed aggregation followed by a de-aggregation phenomenon is similar to those observed in the previous studies on FGA.[7a] This could be explained by the frame–frame interactions (mediated by the interaction between LHGs on the surface of different frames) and then the frame–PA interactions. After the LHGs are anchored to the DNA cuboid scaffold, the hydrophobic interactions between the LHGs are amplified by the presence of multiple interacting sites extended on each surface of the origami cuboid, which caused strong frame–frame associations.[11] Although the introduction of OEG tails on the LHG used here could inhibit the self-assembly of the individual DDOEG molecules, the local high concentration of LHGs on the DNA scaffold would cause the frame to display strong amphiphilic properties, leading to aggregation and precipitation (Supporting Information, Figure S2b). The compatibility and structural/geometry matching of the PA (G_2Cl-18) and the LHG (DDOEG) molecules promote the frame–PA interactions, which are stronger than the frame–frame and PA–PA interactions. Therefore, the addition of G_2Cl-18 molecules would break the frame aggregates, and then the G_2Cl-18 molecules are allowed to further assemble along the sides of the LHGs, resulting in the formation of the hetero-vesicles supported by the cuboid frame (Supporting Information, Figure S2c).[7a,8]

The morphology of the assemblies was examined by TEM to confirm the mechanism described above. After the hybridization of D_TDOEG and the DNA scaffold, only the aggregates were observed in the TEM image with the negative stain of uranyl acetate (Figure 2b), which is consistent with the agarose gel results (Supporting Information, Figure S1). The cuboid shape of the DNA origami scaffold could be identified at the edges of the aggregates, which also indicated that the frame structure was constructed based on the DNA origami scaffold as expected. After the addition of G_2Cl-18 and the annealing procedure, the aggregates disappeared, and only well dispersed cuboid assemblies were found by TEM (Figure 2c). In the magnified image (Figure 2d), a clear corona around the DNA cuboid was observed, which should represent the G_2Cl-18 molecules assembled around the DNA cuboid. The shape of the corona essentially maintained the cuboid geometry of the underlying scaffold. In combination with the precipitate-dissolving phenomenon and the previous study,[7a] these results confirm the formation

of the designed cuboid hetero-vesicles. It should be noted that because of a minimization of the surface tension, the surfaces of the hetero-vesicle at the edges and vertexes are still smooth and gently curved. Nevertheless, this achievement of a cuboid vesicle assembly is a significant step toward creating complex amphiphilic assemblies with unusual geometries, which is difficult to achieve using traditional scaffold-free amphiphilic assembly strategies.

To further confirm the FGA process, dynamic light scattering (DLS) was used to characterize the dimensions of the assemblies. In the DLS data analysis, it is assumed that all the assemblies in the solution are spherical particles, which means the reported value of the average radius (gyration radius) for these cuboid DNA assemblies only reflects an average of the different dimensions for a non-spherical particle. However, the differences between the measured data should correctly reflect the size changes.[12] As shown in Figure 3a, the initial average radius of cuboid **1** is 16.98 nm. After the incubation of cuboid **1** with D_TDOEG, the average radius increased sharply to 106.9 nm, which is due to the aggregation of the frame structure (Figure 3b) and is consistent with the TEM imaging and gel results (Figure 2b).

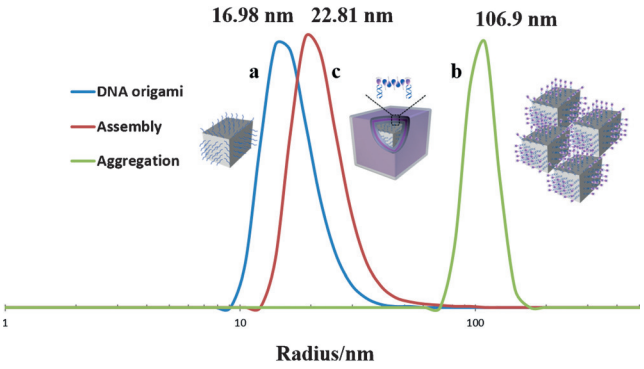

Figure 3. DLS characterization. a) Cuboid **1**. b) The frame aggregates formed by the hybridization of cuboid **1** and D_TDOEG. c) Hetero-vesicles formed by the addition of 5 μM G_2Cl-18.

With the addition of G_2Cl-18 and after the annealing procedure, the average radius of the assemblies decreased to 22.81 nm (Figure 3c), suggesting the aggregation was well dispersed. Compared with cuboid DNA scaffold, the approximately 5.8-nm increase in the radius of the hetero-vesicles confirms the existence of another layer of molecules around the scaffold, which is consistent with the corona in the TEM images (Figure 2c), providing further evidence for the FGA process of G_2Cl-18.

We also took advantage of the versatility of the design strategy of DNA assembly and constructed a cuboid **2** structure, on which only approximately half of the surfaces were modified with the polyA strands (As illustrated in the Supporting Information, Figure S4a). With the one side of cuboid **2** containing the helical ends of the multi-helix structure left as a blunt end, cuboid **2** tends to form a dimeric structure through the π–π stacking of the blunt ends of the DNA duplexes. After hybridization with D_TDOEG and the addition of G_2Cl-18, a dumbbell-shaped assembly with cuboid **2** as the DNA scaffold resulted. In the experiments, a similar precipitate-dissolved phenomenon was observed during the FGA process. It was found by TEM that, compared with the cuboid shape of the DNA scaffold (Supporting Information, Figure S4b), the final assembly shows a well-defined dumbbell morphology (Supporting Information, Figure S4c). These results further verify the shape independence of the FGA process, and it is the arrangement of the leading hydrophobic groups that outline the frame structure that determines the final morphology of the hetero-vesicles.

To demonstrate the general application of the DNA scaffold-based FGA process, different types of LHG and PA were used successfully to form hetero-vesicles of different chemical compositions. As we discussed previously, to guide the assembly of a certain PA, the LHG should be designed carefully. Herein, in addition to the dendron DDOEG/G_2Cl-18 system, we applied two other molecular systems to the FGA process, including small surfactant molecules and thermally sensitive polymers.

As illustrated in Figure 4a, using a lipid (1,2-*O*-dioctadecyl-*rac*-glycerol) molecule with double hydrophobic tails as the LHG, small simple surfactant molecules and sodium dodecyl sulfate (SDS) can be applied to the FGA process. Following a similar assembly procedure as described above, we observed the sequential aggregation of the frame upon the addition of the polyT-linked lipid and the re-dispersion of the DNA cuboid upon the addition of free SDS (Figure 4b,c). On the other hand, with a thermo-responsive poly(propylene oxide) (PPO; M_n, 2000) as the LHG, which would turn hydrophobic when the temperature is higher than the low critical solution temperature, the liner block copolymer R18-b-PPO (M_n, 7550) was guided to form the hetero-vesicles around the frame following the same FGA process, as illustrated in Figure 4d. Without the addition of R18-b-PPO, the frame would self-aggregate when the temperature was raised to 37 °C (Figure 4e); however, upon co-assembly with R18-b-PPO, a well-dispersed cuboid assembly was observed in the TEM images (Figure 4f). Both results

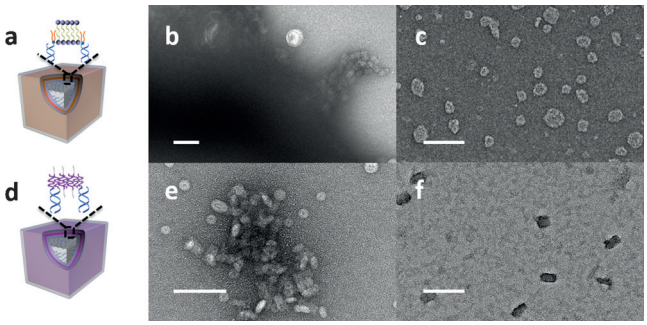

Figure 4. The modularity of this frame-guided assembly process was verified by introducing different combinations of the LHG and the principal amphiphile system. a) A schematic of the lipid–SDS system. b) The aggregates of the frames formed by the hybridization of the cuboid DNA scaffold and the DNA-lipid. c) With the addition of SDS, the aggregates of the frame dispersed. d) The schematic of the PPO-PPO system. e) The TEM image of the aggregates of frames with PPO as the LHG at 37 °C. f) The co-assembly with PPO-R18 of the frame at 37 °C resulted in the well-dispersed DNA structures. Scale bars = 100 nm.

validate the generality of the FGA and show that it is an efficient and powerful tool to control the self-assembly processes of very different amphiphiles, ranging from small surfactant molecules and dendrons to block copolymers.

In conclusion, by employing DNA origami cuboids as model scaffolds, we successfully applied DNA nanotechnology to FGA to control the self-assembly process of amphiphiles. Differently shaped amphiphilic assemblies, including cuboid and dumbbell hetero-vesicles, were constructed by simply adjusting the geometry of the DNA scaffolds and the directed distribution of the LHG on the surfaces of the DNA scaffolds. By carefully choosing different types of LHGs, a wide variety of amphiphiles were confirmed to follow the FGA rules, which proves the generality of FGA. We anticipate that by using FGA it would be possible to construct asymmetric and/or dynamic amphiphilic assemblies with more complex DNA-assembly scaffolds.

Acknowledgements

We thank the National Basic Research Program of China (973 program, no. 2013CB932803), the National Natural Science Foundation of China (nos. 91027046 and 21121004), and NSFC-DFG joint project TRR61 for financial support.

Conflict of interest

The authors declare no conflict of interest.

Keywords: amphiphiles · DNA nanotechnology · frame-guided assembly · self-assembly

How to cite: *Angew. Chem. Int. Ed.* **2017**, *56*, 1586–1589
Angew. Chem. **2017**, *129*, 1608–1611

[1] D. Danino, Y. Talmon, H. Levy, G. Beinert, R. Zana, *Science* **1995**, *269*, 1420–1421.
[2] L. Y. Wang, Y. Feng, Y. W. Sun, Z. B. Li, Z. Q. Yang, Y. M. He, Q. H. Fan, D. S. Liu, *Soft Matter* **2011**, *7*, 7187–7190.
[3] B. N. Thomas, C. R. Safinya, R. J. Plano, N. A. Clark, *Science* **1995**, *267*, 1635–1638.
[4] D. E. Discher, A. Eisenberg, *Science* **2002**, *297*, 967–973.
[5] a) E. A. Guggenheim, *Thermodynamics*: *An Advanced Treatment for Chemists and Physicists*, *8th ed.*, Elsevier, Amsterdam, **1986**; b) I. Müller, *A History of Thermodynamics*: *The Doctrine of Energy and Entropy*, Springer, Berlin; New York, **2007**.
[6] a) M. S. Bretscher, M. C. Raff, *Nature* **1975**, *258*, 43–49; b) A. A. Spector, M. A. Yorek, *J. Lipid Res.* **1985**, *26*, 1015–1035; c) T. P. Stossel, J. Condeelis, L. Cooley, J. H. Hartwig, A. Noegel, M. Schleicher, S. S. Shapiro, *Nat. Rev. Mol. Cell Biol.* **2001**, *2*, 138–145.
[7] a) Y. Dong, Y. Sun, L. Wang, D. Wang, T. Zhou, Z. Yang, Z. Chen, Q. Wang, Q. Fan, D. Liu, *Angew. Chem. Int. Ed.* **2014**, *53*, 2607–2610; *Angew. Chem.* **2014**, *126*, 2645–2648; b) Z. Zhao, C. Chen, Y. Dong, Z. Yang, Q. H. Fan, D. Liu, *Angew. Chem. Int. Ed.* **2014**, *53*, 13468–13470; *Angew. Chem.* **2014**, *126*, 13686–13688; c) Y. Dong, Z. Yang, D. Liu, *Small* **2015**, *11*, 3768–3771.
[8] a) Y. Dong, D. Liu, *Chem. Eur. J.* **2015**, *21*, 18018–18023; b) S. D. Perrault, W. M. Shih, *ACS Nano* **2014**, *8*, 5132–5140; c) A. Czogalla, D. J. Kauert, H. G. Franquelim, V. Uzunova, Y. Zhang, R. Seidel, P. Schwille, *Angew. Chem. Int. Ed.* **2015**, *54*, 6501–6505; *Angew. Chem.* **2015**, *127*, 6601–6605; d) Y. Yang, J. Wang, H. Shigematsu, W. Xu, W. M. Shih, J. E. Rothman, C. Lin, *Nat. Chem.* **2016**, *8*, 476–483.
[9] a) J. C. Mitchell, J. R. Harris, J. Malo, J. Bath, A. J. Turberfield, *J. Am. Chem. Soc.* **2004**, *126*, 16342–16343; b) M. M. Shih, J. D. Quispe, G. F. Joyce, *Nature* **2004**, *427*, 618–621; c) P. W. Rothemund, *Nature* **2006**, *440*, 297–302; d) S. M. Douglas, H. Dietz, T. Liedl, B. Högberg, F. Graf, W. M. Shih, *Nature* **2009**, *459*, 414–418; e) D. Han, S. Pal, J. Nangreave, Z. Deng, Y. Liu, H. Yan, *Science* **2011**, *332*, 342–346; f) D. S. Liu, E. J. Cheng, Z. Q. Yang, *NPG Asia Mater.* **2011**, *3*, 109–114; g) Y. Ke, L. L. Ong, W. M. Shih, P. Yin, *Science* **2012**, *338*, 1177–1183; h) T. Zhou, P. Chen, L. Niu, J. Jin, D. Liang, Z. Li, Z. Yang, D. Liu, *Angew. Chem. Int. Ed.* **2012**, *51*, 11271–11274; *Angew. Chem.* **2012**, *124*, 11433–11436.
[10] Y. Ke, S. M. Douglas, M. Liu, J. Sharma, A. Cheng, A. Leung, Y. Liu, W. M. Shih, H. Yan, *J. Am. Chem. Soc.* **2009**, *131*, 15903–15908.
[11] a) J. N. Israelachvili, D. J. Mitchell, B. W. Ninham, *J. Chem. Soc. Faraday Trans. 2* **1976**, *72*, 1525–1568; b) M. Mammen, S.-K. Choi, G. M. Whitesides, *Angew. Chem. Int. Ed.* **1998**, *37*, 2754–2794; *Angew. Chem.* **1998**, *110*, 2908–2953; c) T. G. Edwardson, K. M. Carneiro, C. K. McLaughlin, C. J. Serpell, H. F. Sleiman, *Nat. Chem.* **2013**, *5*, 868–875.
[12] B. J. Berne, R. Pecora, *Dynamic Light Scattering*: *with Applications to Chemistry*, *Biology*, *and Physics*, Dover, Mineola, **2000**.

Manuscript received: October 16, 2016
Revised: November 16, 2016
Final Article published: December 30, 2016

